

# Accumulated Lifetimes in Single-Axis Vibration Testing

Adam Bouma<sup>1</sup>, Abigail Campbell<sup>2</sup>, Thomas Roberts<sup>3</sup>, Stuart Taylor<sup>4</sup>, Colin Haynes<sup>4</sup>, Dustin Harvey<sup>4</sup>

<sup>1</sup> Department of Mechanical Engineering  
New Mexico State University, Las Cruces, NM 88003

<sup>2</sup> Department of Mechanical Engineering  
University of Utah, Salt Lake City, Utah 84112

<sup>3</sup> Department of Mechanical Engineering  
Rose-Hulman Institute of Technology, Terre Haute, IN 47803

<sup>4</sup> Los Alamos National Laboratory, Los Alamos, NM 87545

## Abstract

Vibration qualification testing verifies and quantifies a system's longevity in its proposed service environments. Service environments a system could encounter can impart many ranges of excitation in all directions; however, multi-axis excitation testing capabilities for simulating realistic environments are rare and costly. Therefore, multiple, single-axis vibration tests are commonly used to qualify a system and its components to a lifetime of service environments. Quantifying the equivalent amount of time a component has been tested can be difficult when limited to single-axis tests. Further complications arise due to the fact that real-world service conditions are often measured at a system level without instrumentation on each component. In addition, many mechanical systems include joints and contact surfaces that, if altered, can significantly change the component's vibration characteristics. This makes replicating the boundary conditions of each component difficult. Therefore, another crucial part of single-axis vibration testing is determining boundary conditions to replicate best the real-world environment onto each component. This paper aims to analyze the effects on lifetime estimates using single-axis vibration testing of components under variations in boundary conditions, testing strategies, control locations, and other configuration options. Methods such as power spectral density (PSD), fatigue damage spectrum (FDS), and Miner's Rule, with quantities such as fatigue cycles, peak response, and RMS response are used to evaluate boundary conditions, study the response of the components, and determine the severity of various test strategies as it pertains to the overall lifetime of the system.

**Keywords:** Vibration, Fatigue, Lifetime, Boundary conditions, Single-axis

## 1. Introduction

Vibration testing using shaker excitation is a common method for qualifying systems and their components when placed in certain service environments. However, it is difficult to replicate the multi-axis test environment in a lab setting. This shortcoming is commonly addressed by sequentially vibrating the system and/or its components on a linear shaker in each primary direction [1]. This single-axis vibration method is easy to perform, widely used, and typically assumed to be equivalent to the multi-axial service environment [2]. However, because of the cross-axis responses that occur when a structure is excited in a single direction, it can be difficult to quantitatively evaluate the service life imposed by multiple, single-axis tests. The lifetime of vibration environments can be calculated in several ways, including power spectral densities (PSD) [3], extreme response spectrums (ERS) [4], fatigue damage spectrums (FDS) [5], as well as taking the peak and root mean square (RMS) [6] of the acceleration time histories. The peak and RMS of the acceleration are scalar values, while the PSD, ERS, and FDS are spectral measures that are each quantified with a specific scalar, as discussed later in the paper in sections 3.3, 3.4, and 3.5. Using a scalar such as a peak provides insight into instantaneous brittle failure, while scalars such as the RMS help to quantify ductile failure. Each of these lifetime definitions can vary from the others and cause further uncertainty when estimating the lifetime imposed on the system.

Additionally, because the boundary conditions in the laboratory usually differ from those in the service environment, it can be difficult to replicate a system's service environment response. In any given system, boundary conditions can include contact surfaces and joints, which can significantly affect responses when altered. Such discrepancies may result in inaccurate stress states and missed failure modes [2], which will ultimately lead to an undesirable amount of life imposed on the system, especially at locations away from the control location. In addition, the boundary conditions tend to change when testing a component of a system on its own [7], which creates more opportunity for inaccuracy when applying system-level measurements to a single-component test.

Finally, it is not always possible to obtain the data from the service environment that is pertinent to the component of interest. It can be difficult to instrument every component within the system due to limited instrumentation, space, or data acquisition capabilities. Thus, it becomes necessary to estimate the response of the component through data that is not specific to the component of interest. This adds another layer of unreliability to the lifetime imposed on the component.

## 2. Experimental Setup

### 2.1 Structure

The structure that was used for this experiment was the Box Assembly with Removable Component (BARC) (Figure 1) developed at Sandia National Laboratories and Kansas City National Security Campus for the Boundary Condition Round Robin Challenge [8]. This structure was specifically developed to provide a common test bed for researchers to use when designing environmental shock and vibration tests and addressing the challenges in determining the “appropriate boundary conditions and input stimulus required to qualify a product” [8]. The structure consists of a partial aluminum box channel subassembly and removable component bolted to the top of the box.

### 2.2 Instrumentation

Acceleration measurements were used for control and data analysis. The entire system included six tri-axial accelerometers. Figure 1 shows the placement of the different sensors on the component and the box respectively. Accelerometers 1, 2, and 6 were placed on the box, while accelerometers 3, 4, and 5 were placed on the removable component. Accelerometers 5 and 6 were used at different times for closed-loop test control, while accelerometers 1-4 were used primarily for response characterization. In Figure 1, accelerometers 1 and 4 are out of view on the opposite side of the structure. Initially, three rosette strain gages were placed at locations 3, 4, and 5; however, the service environment strain data did not exhibit a sufficient signal to noise ratio, so all strain information was neglected in this paper.

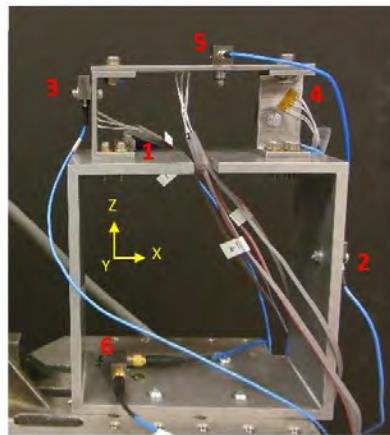


**Figure 1.** Box and Removable Component (BARC) fixture used in this paper and placement of sensors on the component (3, 4, 5) and the box (1, 2, 6).

### 2.3 Boundary Condition Variations

One limitation of single-axis vibration testing is the difficulty of recreating service boundary conditions in the lab environment. Component-level tests in a lab are often performed with rigid attachment to a shaker table, which contrasts with more flexible boundary conditions likely to be seen when the component is assembled in the system. For this experiment, two types of boundary conditions are used to study the effects varying boundary conditions can have on the severity of the single-axis tests. The first boundary condition has the component attached to the box portion of the BARC; this boundary condition will be referred to as flexible and can be seen in the left-hand portion of Figure 2. The flexible boundary condition provides a flexible base when compared to the second, more rigid boundary condition studied in this experiment. The latter will be referred to as the rigid boundary condition and can be seen in the right-hand portion of Figure 2. The rigid boundary condition is a rigid aluminum base that is used to attach the component directly to the shaker table.

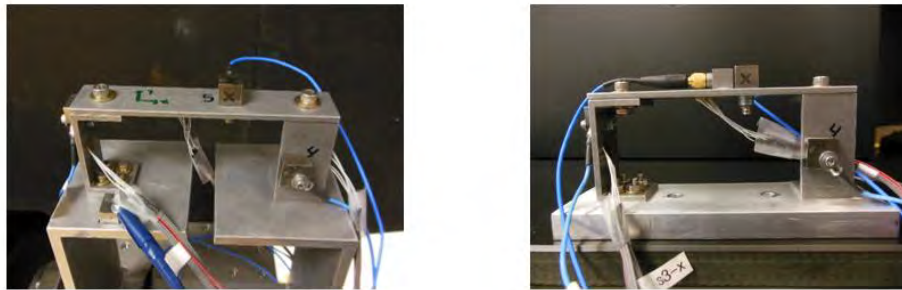


**Figure 2.** Flexible boundary condition (left) and rigid boundary condition (right).

### 2.4 Service Environment

A service environment is any real environment a system is expected to withstand during the system's service life. For this experiment, the service environment was generated with random input to the system in three axes. The responses of the fully instrumented system were recorded to be used as control and comparison data for future tests and analyses. Figure 3 depicts the configuration of the system and three single-axis inputs to generate the service environment.

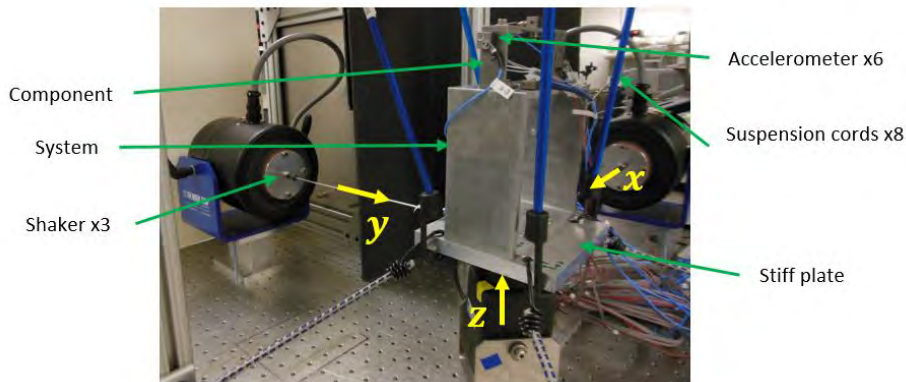


**Figure 3.** Service environment equipment set up consisting of the fully instrumented system, support structure, and three single-axis shakers.

One important aspect of the service environment set up is the boundary condition for the box portion of the system. By fixing the system to a stiff plate, the system is isolated from any unwanted forces from the suspension cords. In addition, this boundary condition is similar to when the system is fixed to the shaker table; using this boundary condition removes one more level of inconsistency from the testing strategies.

### 2.5 Service Environment Data Limitations

Often when performing field tests to obtain data on the service environment of a system, data is not obtained from every component of interest. Absence of component data could be due to lack of sufficient data acquisition capability or the inability

to physically instrument a component to measure its response. In order to test the effects of this data limitation, two control accelerometers at locations 5 and 6 were utilized. Accelerometer 5 was placed at the top of the component and measured the component's response to the service environment. Accelerometer 6 was placed at the base of the subassembly and measured the ground response to the service environment. These two data sources were then used as control input locations for different single-axis tests.

If instrumentation is lacking on a component of interest, it may be necessary to perform an intermediate test to obtain a derived version of the service environment; this process is outlined in Figure 4. This intermediate system-level test is controlled by the data obtained in the original service environment at a measured location not on the component, and then measures the response of the component. Once the component data is obtained, it is then used to control the subsequent component-level tests. In this experiment, service environment data from location 6 was used to control three single-axis intermediate tests at the system level. The component's response at location 5 was recorded in the excited directions to serve as the derived service environment for use in future tests, thus the system-level data can be transferred from the base location at accelerometer 6 up to the component at accelerometer 5.

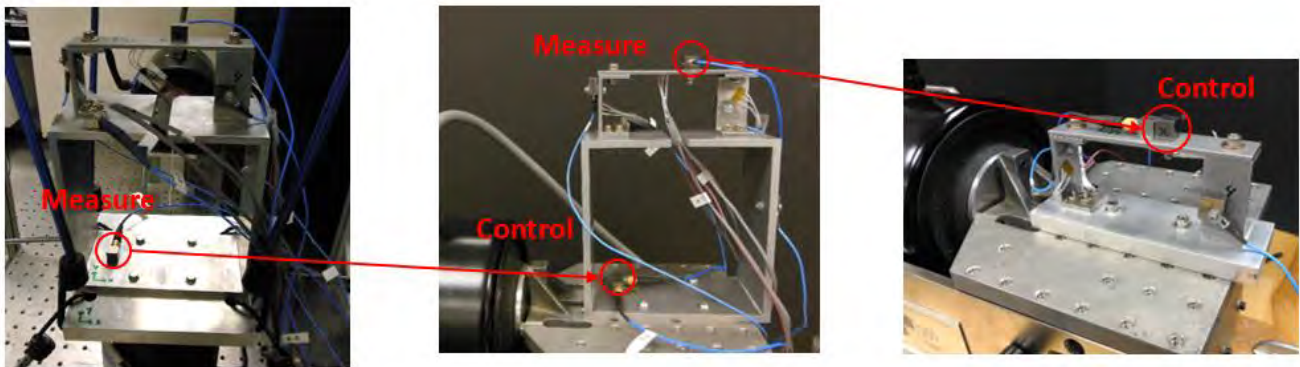


**Figure 4.** Flow of data through the intermediate test to obtain the derived service environment. The response is measured at accelerometer location 6 and is used to control the intermediate test. The response to that test is measured at accelerometer location 5 and then used to control the component test.

## 2.6 Controlled Single-Axis Tests

All single-axis tests were controlled by power spectral density data taken from the service environment or the derived service environment. Four groups of single-axis tests were conducted with each group consisting of three tests, one test in each axis. Table 1 summarizes the four groups of tests and their distinguishing characteristics. Note that component responses from test group 2 serve as the derived service environment used to control test group 4.

**Table 1.** Details of the four different single-axis test groups.

Test Group	Boundary Condition	Control Location	Control Data
1	Flexible	Component (a5)	Service Env. (a6)
2	Flexible	Box (a6)	Service Env. (a6)
3	Rigid	Component (a5)	Service Env. (a5)
4	Rigid	Component (a5)	Derived Service Env. (a5)

Each group of tests provides a specific change in the testing strategy that allows conclusions to be drawn about which aspects of single-axis vibration testing are most significant. Test groups 1 and 2 utilize the box subassembly of the BARC to look at the effects of flexible boundary conditions. Group 1 is controlled using data directly from the component at control location 5. Group 2 is controlled using data from the base of the system at control location 6. Figure 5 shows the experimental setup for system level tests in groups 1 and 2.

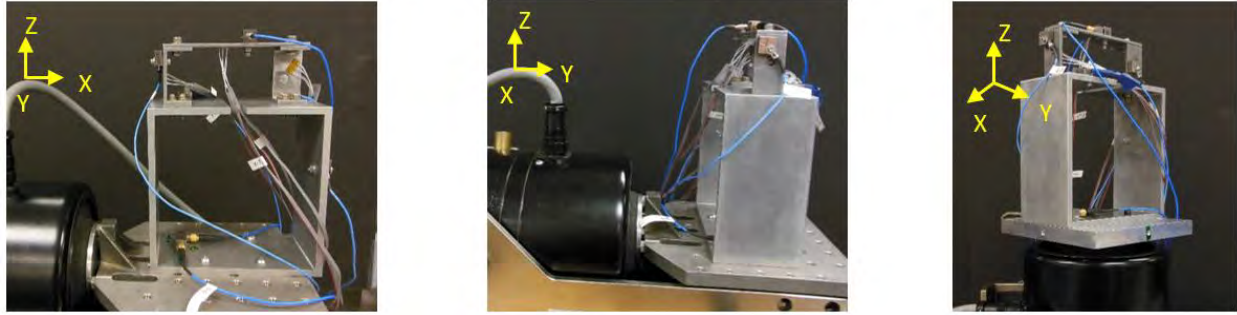


**Figure 5.** Experimental setup for three single-axis flexible boundary condition tests (test groups 1 and 2) for the x (left), y (center), and z (right) excitation axes.

Test groups 3 and 4 are performed using the rigid boundary conditions. Test group 3 is controlled using service environment data at control location 5 while test group 4 is controlled using the derived system data that was described in section 2.5. Figure 6 shows the experimental setup for component level tests in groups 3 and 4.

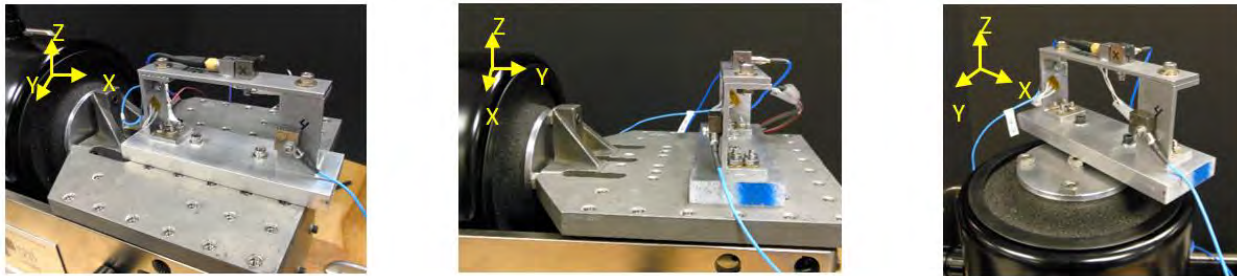


**Figure 6.** Experimental setup for three single-axis rigid boundary condition tests (test groups 3 and 4) for the x (left), y (center), and z (right) excitation axes.

Through this test strategy, it is possible to look at the effects of changing boundary conditions by comparing test groups 1 and 3 and the effects of changing the data source by comparing test groups 3 and 4. Comparison between groups 1 and 2 also illustrates the effects of changing data source, however this paper will focus on test groups 3 and 4, while test group 2 will be used solely for generating the derived service environment. The next section discusses how using different lifetime definitions allows comparison of strategies for estimating lifetime.

### 3. Methods

Cross-axial responses are present during a single-axis vibration test, and they must be considered in a rigorous estimation of the imposed lifetime. To compare the lifetime of a test to the service environment, the test cases must be combined to account for cross-axial responses of the system/component. This can be done by using Palmgren-Miner Rule (Miner's Rule) which is expressed by an inverse power rule as

$$\frac{t_{test}}{t_{service}} = \left( \frac{S_{service}}{S_{test}} \right)^m. \quad \text{Equation (1)}$$

Here,  $t$  is the duration of a test,  $S$  is the severity of a test, and  $m$  is the exponent relating to the material and damage measure [8]. This inverse power rule determines the severity ratio between the service environment and the test environment. In this paper, Miner's Rule was used to combine multiple tests when the severity measure involves power spectral density. All tests were the same length in this experiment, so severity ratios based on PSDs were used as the scalars to combine multiple tests. In the following sections, different measures of test severity are discussed.

### **3.1 Peak of time history**

The peak of a time history can be quickly calculated from an acceleration time history. The peak response of a signal can be acquired by finding the maximum of the absolute value of a signal. This measure can be compared between the service environment and the various test cases to obtain a severity ratio.

### **3.2 RMS of time history**

The RMS of a time history can be calculated quickly from an acceleration time history as well. The RMS values of the service environment and test cases can be compared to obtain a severity ratio. In order to combine multiple tests of different severity, Miner's Rule can be implemented with the severity ratios calculated with each individual RMS value.

### **3.3 Power Spectral Density (PSD)**

The power spectral density is the average power of a signal as a function of frequency. This measure is often used to control vibration tests. The PSD can be calculated in order to determine the severity of each test. Miner's Rule can be applied to combine the like-direction responses to each axis of single-axis testing. An "equivalent" PSD can be calculated and compared to the service environment PSD. To create an equivalent PSD from multiple signals, the severity ratio PSD value of the tests and the service environment at every frequency can be recorded. Miner's Rule is then implemented to combine the values of the test PSDs at each frequency. Furthermore, the RMS values from the combined PSD and the service environment can be used to calculate a severity ratio. These severity ratios will show which test set is the most severe compared to the service environment as well as clarify any over and under testing.

### **3.4 Fatigue Damage Spectrum (FDS)**

The fatigue damage spectrum (FDS) is the cumulative damage as a function of frequency. One method to calculate an FDS is by using the time history response and applying the method proposed by McNeill [5]. In this method, the pseudo-velocity response is calculated followed by a rainflow cycle count. Rainflow counting is a common way to count the number of fatigue cycles a system experiences. This cycle-counting method uses a time domain signal from a vibration test to count full and half cycles and the respective amplitudes of those cycles [10]. The cumulative damage can be computed using Miner's rule and the S-N law. Plotting the cumulative damage vs. the frequency band will yield an FDS. It is important to note that for an FDS it assumes a linear SDOF system and relies on a linear damage accumulation assumption from Miner's Rule. The damping factor and fatigue exponent are also assumed constants.

Once the FDS is computed for the service environment and all test cases, the FDS for each test can be summed according to direction. Since the FDS is a measure of accumulated damage as a function of frequency, multiple FDS's can be summed together as long as the frequency indices remain consistent. To compare these damage measures, the FDS is transformed into a PSD from a method used by McNeill [10]. The RMS values from the FDS generated PSD and the service environment can then be compared via a severity ratio.

### **3.5 Extreme Response Spectrum (ERS)**

The extreme response spectrum (ERS) is defined as the highest peak of the response of a linear SDOF system to the vibration input, according to its frequency for an assumed damping ratio [11]. The response is described by the relative movement of the mass in relation to its support and is closely related to the shock response spectrum (SRS). SRS utilizes a system's highest response during or after a shock, where ERS utilizes the system's maximum response during a longer duration vibration input [12]. The ERS can be calculated either from a time history or from a PSD.

Since the ERS is closely related to the SRS, the method used by Smallwood [13] for calculating the SRS can be applied to calculating the ERS. This method uses a digital recursive filter to simulate a single-degree-of-freedom system. The output of the filter using sampled input is assumed to be a measure of the response of the SDOF system. The response is then searched for the maximum value. This process is repeated for each natural frequency of interest [13].

For this project, the ERS of the service environment and each test were computed from the time history responses. In order to compare severity, the ERSs for all tests were enveloped from like-direction responses. This envelope can then be compared to the service environment ERS. Peaks from the ERS can be observed to obtain the scalar value to produce a severity ratio between the tests and service environment, similar to the RMS values calculated from the PSD.

## 4. Results and Discussion

The results presented in the following sections are comparisons between the service environment and the single-axis test groups described in section 2.2.6 that were intended to reproduce the service environment responses. A severity ratio was computed for each test case, direction, and accelerometer depending on the lifetime measures of interest as described in section 3. All severity ratios are presented in dB scale. A full table of all numeric severity ratios can be found in Table 9 and Figure 17 in Appendix A.

### 4.1 General Results

As a whole, under-testing was uncommon in most testing strategies due to the cross-axis responses to single-axis inputs. The combination of these off-axis responses caused the overall equivalent test to be more severe than the service environment. Figure 7 shows the severity ratios for all test groups at accelerometer locations a3, a4, and a5 using the lifetime measure of RMS of the time history. Each severity ratio in Figure 7 represents the combination of each specific direction's response in all three tests for every test group. The combination of responses is discussed in further detail in section 3. This format is consistent for all following severity ratio figures.

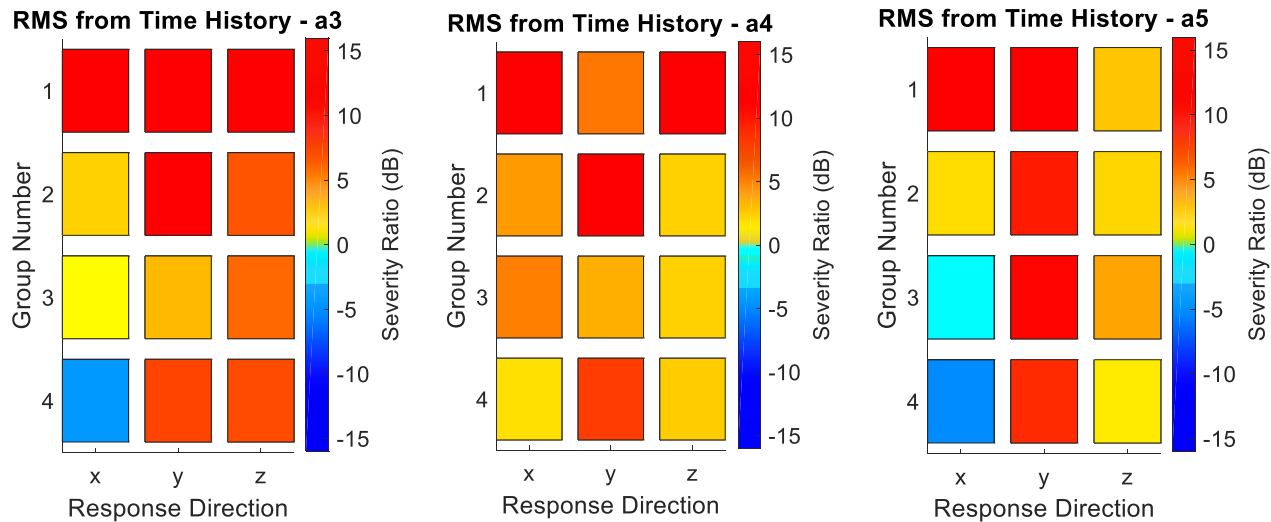


**Figure 7.** Severity ratios based on RMS of the time history for all groups at accelerometer locations a3, a4, and a5. Reference Table 2 in Appendix A for numeric severity ratio values.

The severity ratios for most metrics and groups were greater than one, or 0 dB, which represents a large trend of over-testing. Evidence for this observation can be seen through the power spectral densities from accelerometer location a3 during the three single-axis tests in test group 1, as seen in Figure 8. The off-axis responses for all three input directions were close to or even orders of magnitude larger than the controlled direction responses, which are shown in the Group 1 a5 plots of Figure 8. This was particularly evident in the y and z input directions within a frequency range of 400 to 800 Hz. When all three responses were combined, the overall test severity was often larger than the service environment severity.

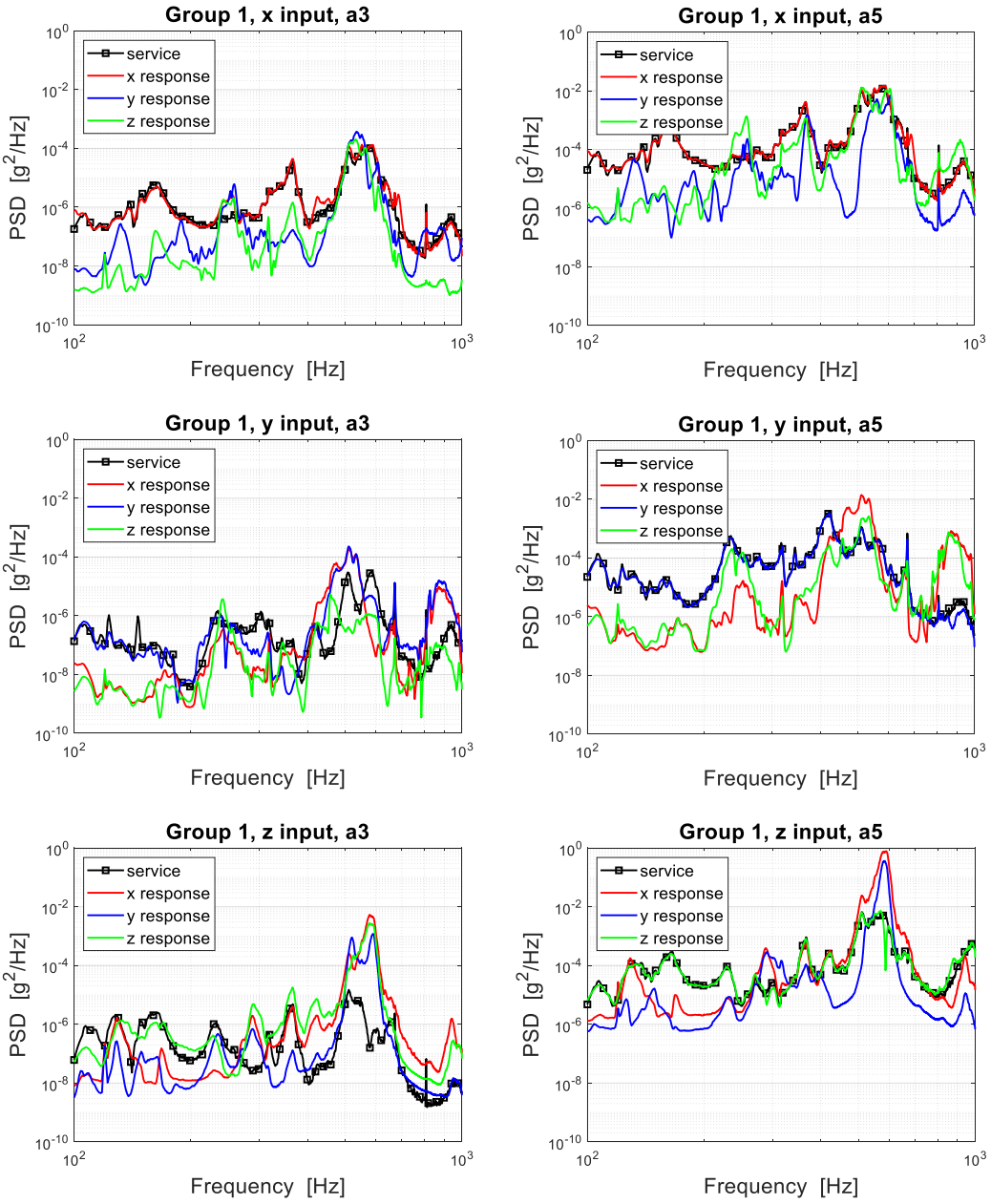


**Figure 8.** PSD of responses to three single-axis inputs for test group 1 at accelerometer locations a3 and a5. Test group 1 was controlled at accelerometer location a5.

Of the four test groups, test group 4 was the only one to show consistent trends of under testing. Test group 4 was controlled with derived service environment data, thus the severity ratios between the test group 4 tests and the service environment were much more susceptible to showing under testing. This can be seen in Figure 9 which shows the power spectral density data for the service and derived service environments at accelerometer location a5.

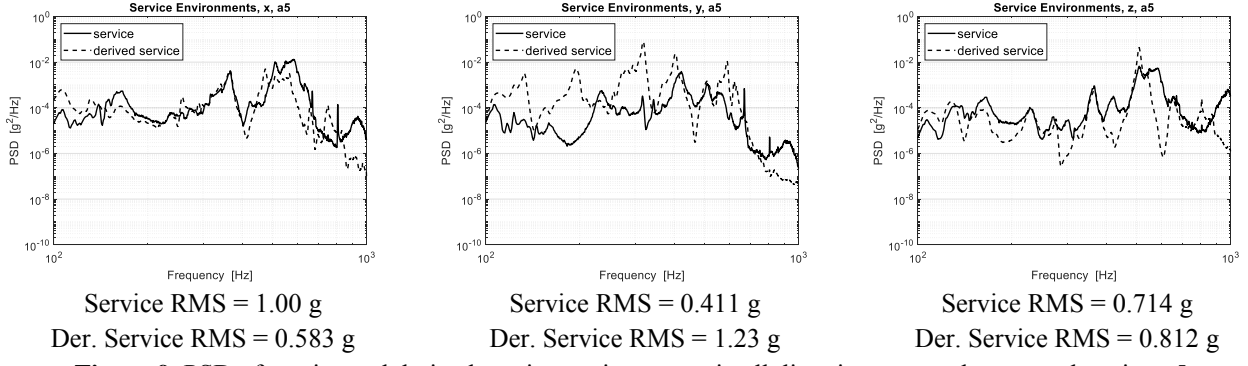


**Figure 9.** PSD of service and derived service environments in all directions at accelerometer location a5.

The derived service environment signal for the x-direction contained significantly less power than the service environment signal. As the x-direction test for test group 4 was controlled to the derived service environment data, we expect to see a fair amount of under testing when comparing to the service environment. Figure 10 shows the severity ratios for all lifetime measures in the x, y, and z-directions for test group 4 at accelerometer location a5. As expected, the x-direction was consistently under tested when compared to the service environment. This trend was consistent in accelerometers locations a3 and a4, and this information can be found in Figure 17 and Table 9 in Appendix A.

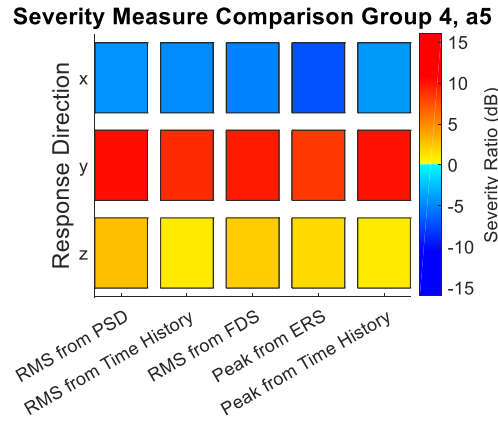


**Figure 10.** Severity ratios for all directions and lifetime measures for test group 4 for at accelerometer location a5. Reference Table 3 in Appendix A for numeric severity ratio values.

It is also clear from Figure 9 that there is significant over testing in the y direction. Analyzing the results from all tests shows this trend of over testing in the y-direction is consistent across all groups and all accelerometers. One instance of this can be seen in the z-input portion of Figure 8, where the y-response to the z-input is nearly two orders of magnitude higher than that of the y-direction service environment. A similar trend can be seen in Figure 11 where the y-direction severity ratios are shown for all groups and all lifetime measures at accelerometer location a3. All groups exhibited significant over testing regardless of the lifetime measure used to assess test severity. The consistency of this result between all groups and lifetime measures suggests that the source of this over testing is not within a testing strategy, but rather due to some feature of the BARC structure in the y-direction. The large difference between the y-direction test severities and the x and z-directions suggests that there is a possibility for large variation in results depending on the response direction of interest.

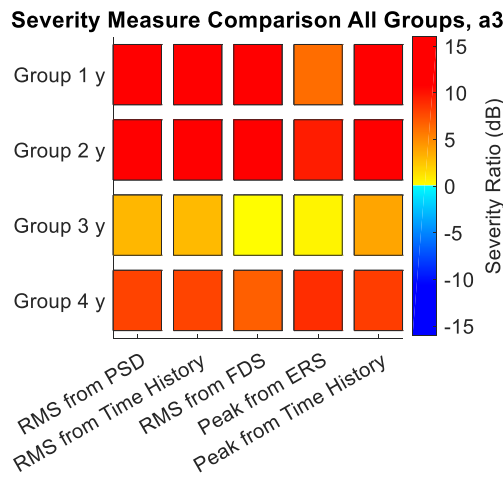


**Figure 11.** Severity ratios in the y-direction for all test groups and lifetime measures at accelerometer location a3. Reference Table 4 in Appendix A for numeric severity ratio values.

Another area of interest in this experiment is the effect on lifetime estimation depending on where the structure is measured. As previously described, each test was controlled at only one location and in one direction. All other measurement locations were likely to exhibit some degree of undesirable behavior, as their responses were not being controlled. As an example, to study these effects the severity ratios for test group 4 at accelerometer locations a3, a4, and a5 are shown in Figure 12. Because test group 4 was controlled with derived service environment data, the severity ratios shown in Figure 12 may not be exactly one, or 0 dB, in the excited directions. The severity ratios across all three measurement locations appear to be rather consistent especially in the x and z response directions. The mean values of severity ratio between the three measurement locations differ by a maximum of 28%. Future results in this section will show that a 28% difference in the mean value of severity ratio is rather insignificant compared to other sources of variation within the testing strategies. With other sources of variability largely outweighing variations due to measurement location, single-axis component test could be controlled at any convenient location and measured elsewhere without much concern of the effects of instrumentation location.

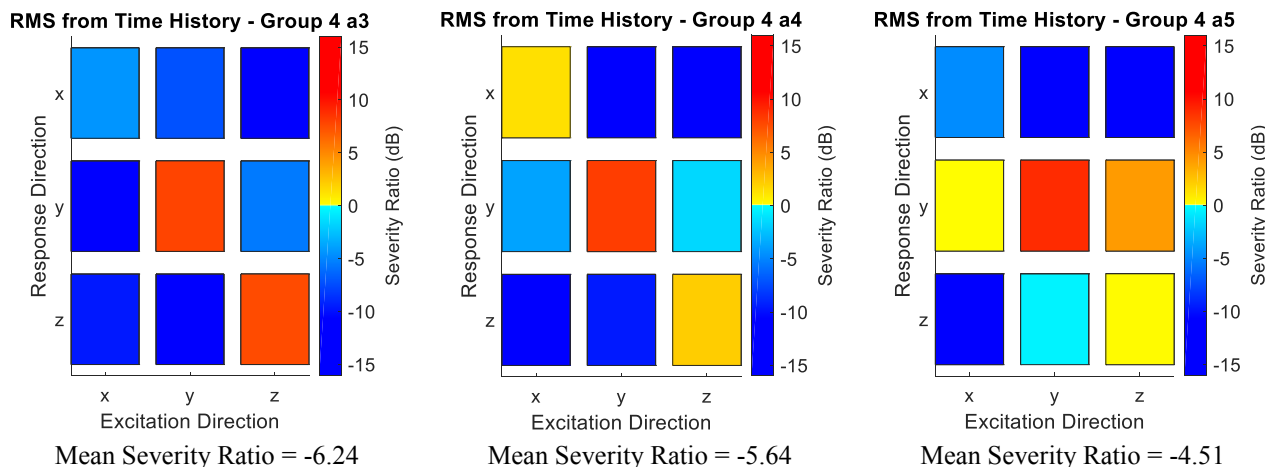


**Figure 12.** Severity ratios based on RMS of the time history for test group 4 at accelerometer locations a3, a4, and a5. Reference Table 5 in Appendix A for numeric severity ratio values.

Other topics of interest in estimating lifetimes are changing the lifetime estimation measure, changing boundary conditions, and changing control data. The following three subsections target each one of these sources of variability in order to assess their effects on the estimate lifetimes imposed on the component.

## 4.2 Changing the Lifetime Estimation Measure

Another notable feature of Figure 10 is the consistency in severity ratios between each different lifetime measure. The rows of Figure 10 show very little variation in their severity ratios, which suggests that all of the lifetime measures considered here provide consistent results. This result holds for nearly all groups, locations, and directions. Figure 13 shows the severity ratios for all lifetime measures for test group 4 at accelerometer locations a3 and a4 – Figure 10 is the last of the set of 3 figures for test group 4. The standard deviations (SD) of the severity ratios for each direction quantitatively show the consistency between the lifetime measures across all measurement locations. This consistency removes the possibility of variability in the results from different lifetime measures. Thus, the majority of the following results will focus on a single lifetime measure.

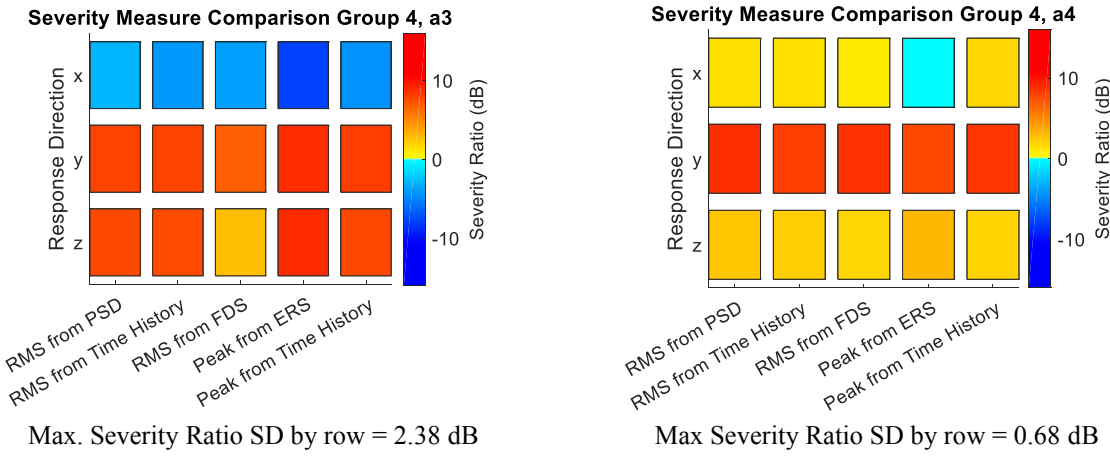


**Figure 13.** Severity ratios for all lifetime measures for group 4 at accelerometer locations a3 and a4. The maximum values for standard deviation (SD) of the severity ratios (by row) are shown below the severity ratio figures. Reference Table 6 in Appendix A for numeric severity ratio values.

## 4.3 Changing Boundary Conditions

Test groups 1 and 3 were used to study the effects of changing boundary conditions on test severity. As mentioned in Table 1, test group 1 utilizes the flexible boundary conditions while controlling the test at accelerometer location a5. Test group 3 utilizes the rigid boundary conditions while still controlling at accelerometer location a5. Of these two groups, test group 3 over-tested less than test group 1. The difference between the groups' severity ratios is significant, as can be seen in Figure 14.

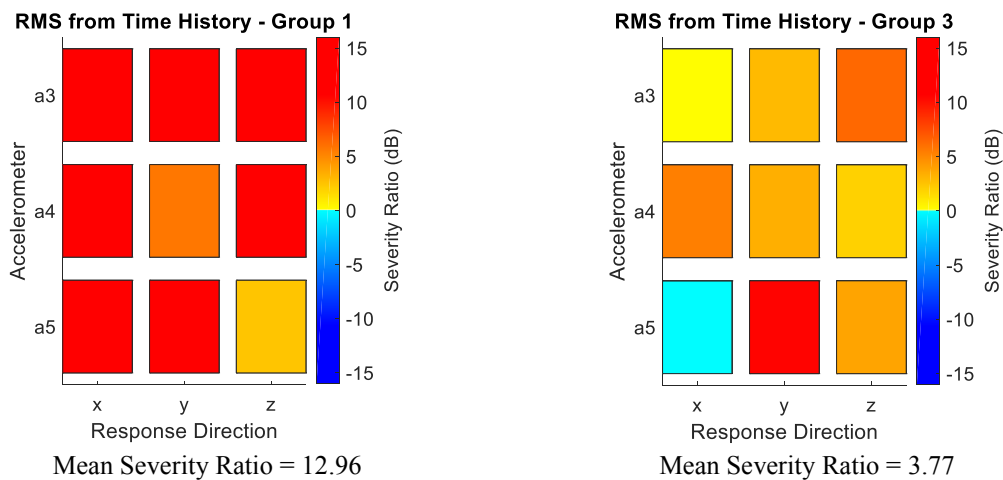


**Figure 14.** Severity ratios based on RMS of the time history for test groups 1 and 3 in all directions and at all accelerometer locations. Reference Table 7 in Appendix A for numeric severity ratio values.

With the exception of the results at accelerometer location a5 in the z-direction, test group 1 always experienced higher severity than test group 3. The mean severity ratios between groups 1 and 3 differ by nearly 70%. In this case, the rigid boundary

conditions in test group 3 allow for better test control than the flexible boundary conditions in test group 1. This result implies that rigid boundary conditions restrict the amount of off-axis response in each single-axis test. Figure 15 shows the power spectral densities from test groups 1 and 3 at accelerometer location a4 when the system was excited in the z-direction. Test group 1 experienced significant off-axis response in the 400 to 800 Hz frequency range, while test group 3 experiences much less off-axis response. The x-direction response to the z-direction input decreased by nearly four orders of magnitude when the boundary conditions were changed from flexible to rigid. The y-direction response to the z-direction input decreased less than the x-direction, but still justifies the claim that the rigid boundary conditions limit the off-axis response in the structure.

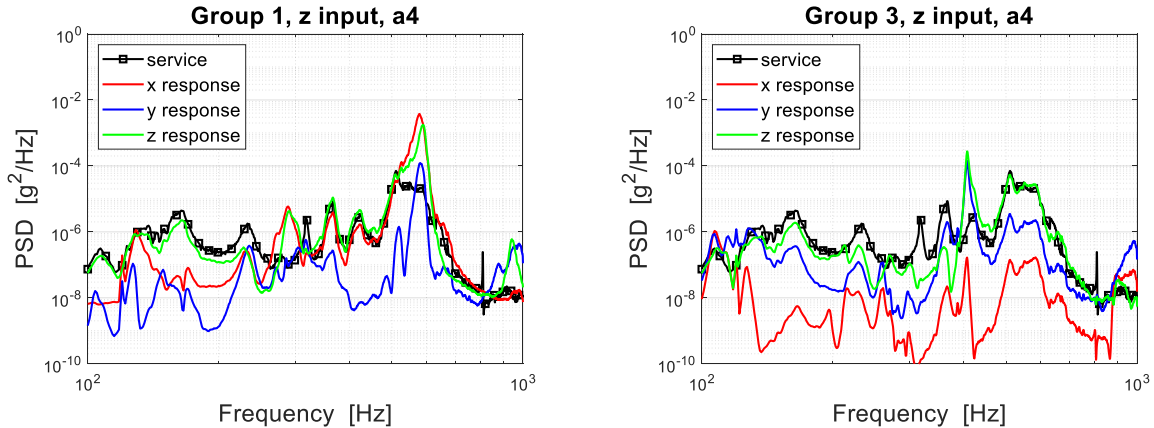


**Figure 15.** PSD of responses to z-axis inputs from test groups 1 and 3 at accelerometer location a4.

#### 4.4 Changing Control Data

Test groups 3 and 4 were used to study on the effects of changing control data on test severity. As mentioned in Table 1, test group 3 utilizes the rigid boundary conditions while controlling at accelerometer location a5 with service environment data. Test group 4 also uses the rigid boundary conditions but instead controls at accelerometer location a5 with derived service environment data. Comparison of the severity ratios from test groups 3 and 4, as shown in Figure 16, yields a 19% difference between the mean severity ratios, suggesting that changing control data has a relatively minimal effect on test severity when compared to the effect of changing boundary conditions. Even though the service environment (used for control in test group 3) is not identical to the derived service environment (used for control in test group 4), the effect on test severity is less significant. Thus, the minimal effect of changing control data is likely due to the role of the rigid boundary conditions reducing the off-axis responses.

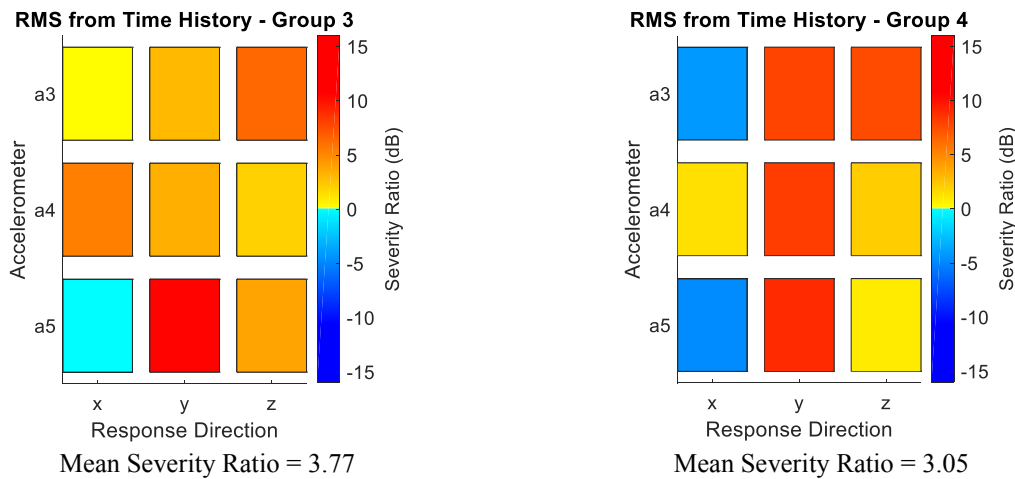


**Figure 16.** Severity ratios based on RMS of the time history for groups 3 and 4 in all directions and at all accelerometer locations. Reference Table 8 in Appendix A for numeric severity ratio values.

## **5. Conclusions**

Different vibration testing strategies were studied through a series of single-axis vibration tests on a structure consisting of a box and a component. The experiments focused on replicating a service environment on the component through previously mentioned test strategies in order to determine their effect on the estimation of the imposed lifetime. Three major changes were made between all of the test groups: changing the lifetime measure, boundary conditions, and control data. Over-testing is common when taking into account the off-axis responses in severity estimations, especially when flexible boundary conditions are used. The y-direction on the BARC structure experienced the most severe tests, which suggests that the estimated lifetime imposed on the system may vary significantly by response direction. Overall, changing the lifetime estimation method had a significantly smaller effect than changing boundary conditions, control data, or measurement location. Of the three main changes to the testing strategies, changing boundary conditions from rigid to flexible had the largest effect on test severity. Changing control data and varying measurement location still had measurable effects on test severity, but their effects were significantly less than changing boundary conditions. For this particular system (BARC), it could be suggested that component level vibration tests be controlled with derived service environment data with little repercussion from the lack of service environment information. Practitioners of other structures could employ this methodology to determine if this BARC-specific conclusion applies to more structures. In addition, component level tests could be fixtured using simple rigid boundary conditions for better test control. Lastly, the tests could be controlled from any easy access point on the component, and the measurements from the non-controlled locations should still be just as valid as the control location.

The next step for this experiment would be to design new tests to drive all severity ratios to unity. Depending on which test group is of interest, different excitations could be scaled in order to make the accumulated lifetime from the test environment match the service environment. Depending on the frequency range of interest, some tests resulted in severity ratios very close to unity. However, in the frequency range of 400 to 800 Hz, this structure would require a significant amount of changes to the control data to reduce the test severity. In addition, the collection of strain data would be an improvement for further characterization the response of any system of interest as well as allowing more methods for estimating the imposed lifetime.

## References

- [1] C. Harman and M. B. Pckel, "Multi-Axis Vibration Reduces Test Time," *Evaluation Engineering*, 2006.
- [2] D. O. Smallwood, "The Challenges of Multiple Input Vibration Testing Analysis," *Sandia National Laboratory*, 2013.
- [3] A. Brandt., *Noise and Vibration Analysis: Signal Analysis and Experimental Procedures*, John Wiley & Sons, 2011.
- [4] G. R. Henderson, *Evaluating Vibration Environments Using the Shock Response Spectrum*, Sound and Vibration, 2003.
- [5] S. I. McNeill, "Implementing the Fatigue Damage Spectrum and Fatigue Damage Equivalent Vibration TEsting," in *Proceedings of the 79th Shock and Vibration Symposium*, Orlando, Florida, 2008.
- [6] K. McConnel, *Vibration Testing: Theory and Practice*, John Wiley & Sons, 1995.
- [7] P. Avitable, "Can test setup have an effect on the measure of modal data?," *Modal Space, In Our Little World*, December 2011.
- [8] D. E. Sione, R. J. Jones, J. M. Harvey, T. J. Skousen and T. Schoenherr, "Deisgning Hardware for the Boundary condition round Robin Challenge," Kansas City National Security Campus; Sandia National Laboratories, 2017.
- [9] C. Lalanne, "Fatigue Damage," *Mechanical Vibration and Shock Analysis: third Addition*, vol. 4, 2014.
- [10] Y. Murakam, "The Rainflow Counting Method in Fatigue," *The Fatsuo Endo Memorial volume: Elsevier Science and Technology*, 2013.
- [11] C. Lalanne, "Specification Devlopment," *Mechanical Vibration and Shock Analysis: Third Edition*, vol. 5, 2014.
- [12] C. Lalanne, "Mechanical Shock," *Mechanical Vibration and Shock Analysis: Second Addition*, vol. 2, 2009.
- [13] D. O. Smallwood, "An improved recursive formula for calculating shock response spectra," *Shock Vib Bull*, vol. 51, pp. 4-10, 1981.

## Appendix A

This appendix contains numeric values pertaining to the severity ration figures presented throughout section 4. All severity ratios are presented in dB scale.

**Table 2.** Severity ratios based on RMS of the time history for all groups at accelerometer locations a3, a4, and a5.

Group Number	RMS from Time History – a3			RMS from Time History – a4			RMS from Time History – a5		
	1	12.858	13.698	21.358	18.508	5.665	11.157	14.128	16.874
2	1.907	11.357	7.082	4.190	11.445	1.935	1.364	9.533	1.629
3	0.045	2.862	6.298	5.311	3.311	1.895	-0.069	10.497	3.785
4	-4.281	7.799	7.533	1.296	8.107	2.078	-4.789	8.882	0.803
	x	y	z	x	y	z	x	y	z
	Response Direction			Response Direction			Response Direction		

**Table 3.** Severity ratios for all directions and lifetime measures for test group 4 for at accelerometer location a5.

Severity Measure Comparison Group 4, a5						
Resp. Dir.	x	-4.401	-4.789	-5.164	-7.162	-4.224
	y	10.063	8.882	9.552	8.245	9.909
	z	2.670	0.803	2.058	1.524	0.778
	RMS from PSD	RMS from Time History	RMS from FDS	Peak from ERS	Peak from Time History	

**Table 4.** Severity ratios in the y-direction for all test groups and lifetime measures at accelerometer location a3.

Severity Measure Comparison All Groups, a3					
Group 1 y	14.414	13.698	11.838	6.055	12.980
Group 2 y	12.760	11.357	11.186	9.499	11.543
Group 3 y	2.992	2.862	0.042	0.408	3.736
Group 4 y	7.853	7.799	6.652	8.708	8.111
	RMS from PSD	RMS from Time History	RMS from FDS	Peak from ERS	Peak from Time History

**Table 5.** Severity ratios based on RMS of the time history for test group 4 at accelerometer locations a3, a4, and a5.

Resp. Dir.	RMS from Time History – Group 4, a3			RMS from Time History – Group 4, a4			RMS from Time History – Group 4, a5					
	x	-4.433	-7.264	-16.719	x	1.296	-15.059	-15.495	x	-4.791	-13.195	-21.751
y	-15.463	7.799	-5.158	y	-3.821	8.106	-1.584	y	0.043	8.841	4.134	
z	-9.633	-12.466	7.533	z	-16.725	-9.573	2.078	z	-13.543	-0.455	0.1424	
	x	y	z	x	y	z	x	y	z			
	Excitation Direction			Excitation Direction			Excitation Direction					

**Table 6.** Severity ratios for all lifetime measures for group 4 at accelerometer locations a3 and a4.

		Severity Measure Comparison Group 4, a3					Severity Measure Comparison Group 4, a4				
Resp. Dir.	x	-2.994	-4.281	3.991	-7.881	4.519	1.317	1.296	0.868	-0.079	1.676
	y	7.853	7.799	6.652	8.708	8.111	8.613	8.107	8.589	7.591	8.355
	z	7.5776	7.533	2.729	8.856	7.608	2.328	2.078	1.627	2.931	1.829
	RMS from PSD	RMS from Time History	RMS from FDS	Peak from ERS	Peak from Time History	RMS from PSD	RMS from Time History	RMS from FDS	Peak from ERS	Peak from Time History	

**Table 7.** Severity ratios based on RMS of the time history for test groups 1 and 3 in all directions and at all accelerometer locations.

Accel.	RMS from Time History – Group 1			RMS from Time History – Group 3			
	a3	12.858	13.698	21.358	0.040	2.862	6.298
	a4	18.508	5.666	11.157	5.311	3.311	1.895
	a5	14.128	16.874	2.398	-0.069	10.497	3.785
	x	y	z	x	y	z	
	Response Direction			Response Direction			

**Table 8.** Severity ratios based on RMS of the time history for groups 3 and 4 in all directions and at all accelerometer locations.

Accel.	RMS from Time History – Group 3			RMS from Time History – Group 4			
	a3	0.040	2.862	6.298	-4.281	7.799	7.533
	a4	5.311	3.311	1.895	1.296	8.107	2.078
	a5	-0.069	10.497	3.785	-4.789	8.815	0.803
	x	y	z	x	y	z	
	Response Direction			Response Direction			

**Table 9.** Severity ratios for all test groups, accelerometers, directions and lifetime measures.

a3x	12.968	12.858	10.368	3.342	9.448	3.005	1.907	2.195	-7.287	0.671	0.593	0.040	-0.497	-0.941	-0.291	-2.994	-4.281	-3.991	-7.881	-4.519
a3y	14.414	13.698	11.838	6.055	12.980	12.760	11.357	11.186	9.500	11.543	2.992	2.862	0.042	0.408	3.736	7.853	7.799	6.652	8.708	8.111
a3z	21.436	21.358	14.390	22.563	19.429	8.300	7.081	2.050	13.742	7.100	6.372	6.298	1.525	5.302	6.750	7.578	7.533	2.729	8.856	7.608
a4x	18.579	18.508	16.977	12.616	16.955	5.751	4.190	4.998	3.583	4.722	5.342	5.311	4.330	6.300	5.200	1.317	1.296	0.868	-0.079	1.676
a4y	6.775	5.666	3.342	4.586	2.406	11.784	11.445	11.962	13.126	11.109	5.397	3.310	5.009	0.991	3.013	8.613	8.107	8.589	7.591	8.355
a4z	12.053	11.157	8.124	14.305	8.226	4.021	1.935	2.364	-1.167	0.730	2.011	1.895	1.800	0.373	1.946	2.328	2.078	1.627	2.931	1.829
a5x	14.181	14.128	11.440	-0.091	11.073	2.431	1.364	1.659	-6.543	0.843	0.262	-0.069	-0.779	-1.177	0.265	-4.401	-4.789	-5.164	-7.162	-4.224
a5y	16.961	16.874	13.931	5.051	14.301	9.853	9.533	9.458	8.434	9.286	10.757	10.497	11.580	9.045	10.935	10.063	8.881	9.552	8.245	9.910
a5z	3.161	2.398	2.243	15.767	2.950	3.574	1.630	2.684	5.074	0.501	4.910	3.785	2.809	8.167	3.437	2.670	0.803	2.058	1.524	0.778
	RMS from PSD	RMS from Time History	RMS from FDS	Peak from ERS	Peak from Time History	RMS from PSD	RMS from Time History	RMS from FDS	Peak from ERS	Peak from Time History	RMS from PSD	RMS from Time History	RMS from FDS	Peak from ERS	Peak from Time History	RMS from PSD	RMS from Time History	RMS from FDS	Peak from ERS	Peak from Time History
	Group 1				Group 2				Group 3				Group 4							

### Severity Measure Comparison All Groups

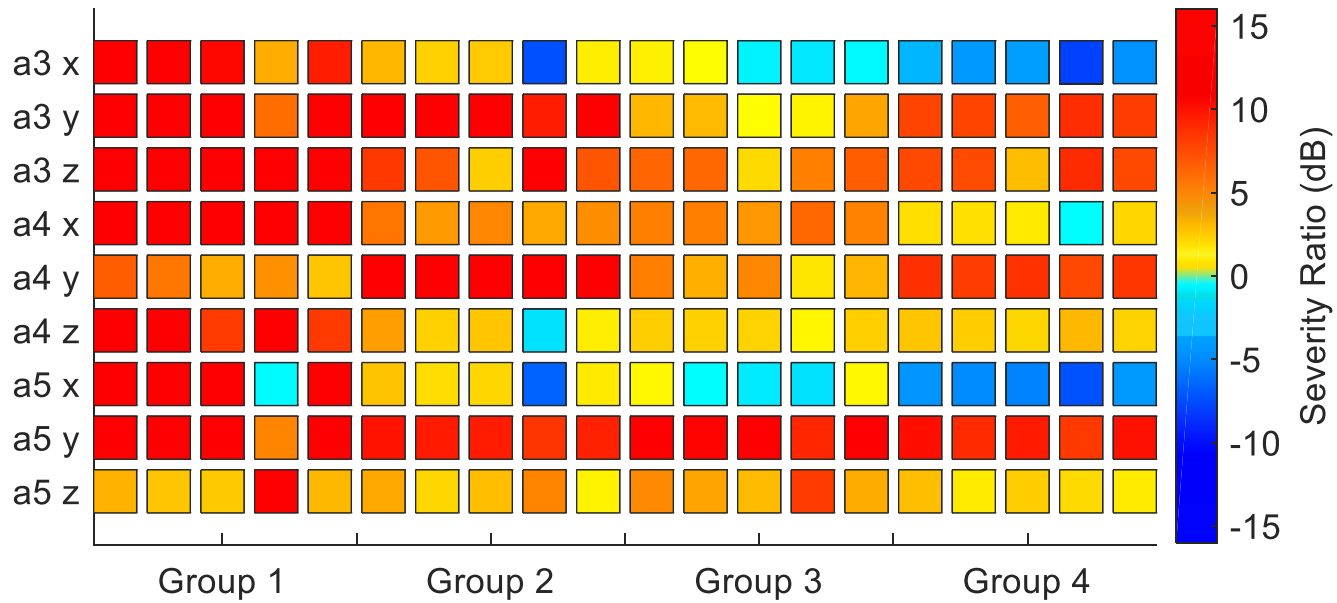


**Figure 17.** Severity ratios for all groups, accelerometers, directions, and lifetime measures. Reference Table 9 for numeric severity ratio value